

# Structural studies on ethylene–tetrafluoroethylene copolymer

## 1. Crystal structure

Tetsuya Tanigami,\* Kazuo Yamaura and Shuji Matsuzawa

Department of Chemistry, Faculty of Textile Science and Technology, Shinshu University, Ueda-shi, Nagano-ken 386, Japan

and Masazumi Ishikawa,† Keishin Mizoguchi‡ and Keizo Miyasaka

Department of Textile and Polymeric Materials, Tokyo Institute of Technology, Ookayama, Meguro-ku, Tokyo 152, Japan

(Received 15 July 1985; revised 2 September 1985)

The crystal structure for an ethylene–tetrafluoroethylene (ETFE) alternating copolymer film containing highly ordered crystal regions was determined. The unit cell is orthorhombic with the dimensions:  $a = 8.57 \text{ \AA}$ ,  $b = 11.20 \text{ \AA}$ , and  $c$  (chain axis)  $= 5.04 \text{ \AA}$ . Four planar zigzag chains are packed in the unit cell. The lateral packing mode is similar to that of orthorhombic polyethylene (PE). A study on the mode of double orientation confirmed that the crystal structure of ETFE, which has been assumed to be pseudo-hexagonal, is indeed orthorhombic as described above, although it has paracrystalline disorder.

(Keywords: ethylene–tetrafluoroethylene copolymer; crystal structure; X-ray diffraction; double orientation; disorder)

### INTRODUCTION

The X-ray diffraction pattern of a drawn ETFE film is known to have only one discrete and intense diffraction spot at  $2\theta = 19^\circ$  on the equator. The other equatorial spots are very weak and the layer line reflections are diffuse. This character of the X-ray pattern has sometimes been related to the irregular alternation of the two monomer units in the chain, as an unavoidable part of the nature of copolymers even if the chains are arranged in their highest order of packing.

Wilson and Starkweather<sup>1</sup> proposed that four planar zigzag chains are placed in either an orthorhombic or monoclinic ( $\gamma = 96^\circ$ ) unit cell with  $a = 9.6 \text{ \AA}$ ,  $b = 9.2 \text{ \AA}$  and  $c = 5.0 \text{ \AA}$ , corresponding to the space group  $Cmca-D_{2h}^{18}$ . They proposed a molecular packing in this unit cell by using a molecular model. Thus, the observed reflection intensity has not yet been compared with the calculated one. By referring to the diffractions obtained with a drawn and rolled sample, they concluded that both 200 and 020 reflections appeared at  $2\theta = 19^\circ$  overlapping with each other. They did not pay attention to a weak reflection at  $2\theta = 21^\circ$  observed on the transverse direction of the sample. These two reflections at  $2\theta = 19^\circ$  and  $21^\circ$  were observed more distinctly than those of Wilson and Starkweather by three other groups<sup>2–4</sup>. These groups did not describe the sample preparations in detail, but probably used powdered samples. As the sample Wilson and Starkweather used was filamented, they probably could not make an X-ray observation of its end-view

pattern. Therefore, they could not exactly comprehend the double orientation mode of the crystallites.

For the perfectly alternating ETFE, Farmer and Lando<sup>5</sup> calculated potential energies of the molecular packing in a unit cell, and proposed three possible packing modes: (i) packing similar to PE; (ii) packing similar to poly(vinylidene fluoride) phase I crystal, and (iii) packing proposed by Wilson *et al.* They found no significant difference in the packing energies of these modes, and suggested that the actual structure may be a mixture of them. However, it should be noticed that rather than the variety of the packing modes expected for the fictitious regular alternating copolymer, the actual irregular alternation of the monomer units in the chain seems more effectively to influence the molecular packing order.

Recently, by melt-extrusion under extension, we prepared a film of ETFE in which crystals are uniaxially oriented and found that two well-separated equatorial reflections at  $2\theta = 19^\circ$  and  $21^\circ$  appear. This sample prompted us to reexamine the crystal structure of ETFE. Here we report the results with some discussion on the anisotropy of the crystal orientation caused by rolling.

### EXPERIMENTAL

#### Samples

The following five ETFE films were used in this study.

*Sample A.* A commercial film 300  $\mu\text{m}$  thick (Aflex, Asahi Glass Co., Japan) was drawn uniaxially six times by using a manually operated device in silicone oil at 200°C. The drawn film was annealed at the fixed length at 200°C for 1 h. The density of sample A was  $1.74 \text{ g cm}^{-3}$ . Figures 1a, b show wide-angle X-ray diffraction (WAXD) and

\* To whom correspondence should be addressed.

† Present address: Central Engineering Laboratories, Nissan Motor Co. Ltd., Natsushima, Yokosuka-shi 237, Japan.

‡ Permanent address: Industrial Research Institute, Yatabe-cho, Tsukuba-gun, Ibaraki-ken 305, Japan.

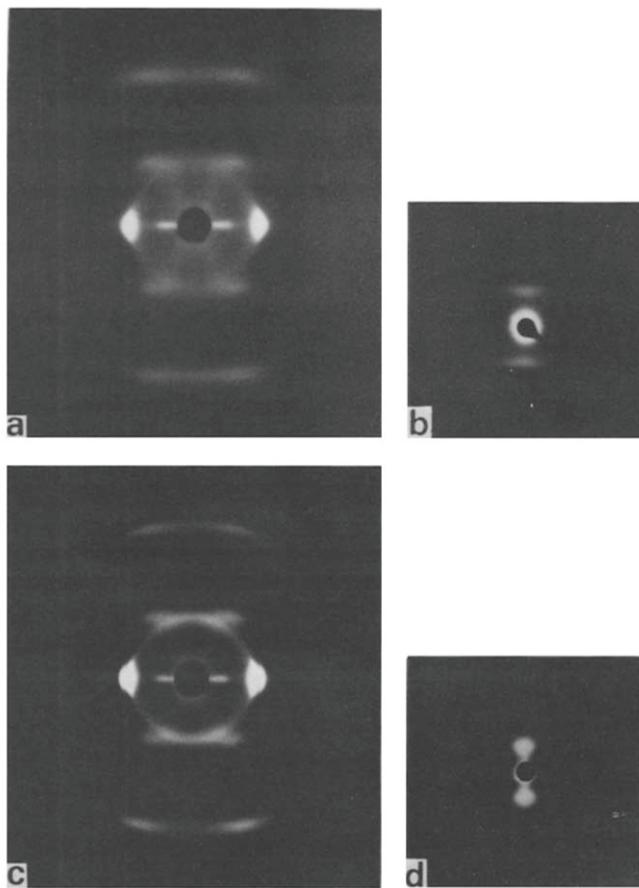


**Figure 1** X-ray diffraction photographs of ETFE: (a) WAXD and (b) SAXS photographs of sample A; (c) WAXD and (d) SAXS photographs of sample B. Drawing direction for sample A and extrusion direction for sample B are vertical

small-angle X-ray scattering (SAXS) photographs of the sample, respectively. *Figure 1a* shows that the crystals are well oriented uniaxially.

**Sample B.** A film 10  $\mu\text{m}$  thick and 20 cm wide was prepared from molten ETFE pellets (Aflon COP, Asahi Glass Co.) by using an extruder equipped with T-die. The melt at 300°C was extruded into the atmosphere at room temperature and taken up at a speed of 18 m min<sup>-1</sup>. This film had a high degree of crystal orientation owing to the tension applied during cooling. To increase the crystallinity, the film was annealed at 200°C for 1 h. The density of the sample was 1.76 g cm<sup>-3</sup>. *Figures 1c, d* show WAXD and SAXS photographs of sample B. The degree of the crystal orientation in sample B is as high as in sample A. *Figure 1d* shows a two-point pattern on the meridian as usually observed in samples prepared by melt-extrusion under high tension. The pattern indicates that lamellar structure is highly developed.

**Sample AR.** The same drawn film as used for sample A was rolled along the drawing direction in a two-roll mill at 180°C, and then was annealed at a fixed length at 200°C for 1 h. The density was 1.73 g cm<sup>-3</sup>.

**Sample R.** The unoriented commercial film Aflex was repeatedly rolled in a given direction in the mill at 180°C. The rolled film was annealed under the same conditions as for samples A and AR. The density was 1.73 g cm<sup>-3</sup>. (The WAXD and SAXS photographs of these rolled films R and AR are shown in *Figures 9* and *10*, respectively.)

### X-ray measurements

Ni-filtered Cu K $\alpha$  radiation (35 kV and 20 mA) was used for WAXD measurements. Photographs were taken with a flat camera with a pinhole of 0.5 mm diameter, and the intensity curves were obtained with a Rigaku-Denki Geigerflex. SAXS photographs were taken with Ni-filtered Cu K $\alpha$  radiation (45 kV and 50 mA) by using a Rigaku-Denki RU-3 rotating-anode generator. Pinholes of 0.3 and 0.2 mm diameter were used as the first and second apertures for the incident beam, respectively.

## RESULTS AND DISCUSSION

### Variation of X-ray diffraction profile with sample preparation

*Figure 1* shows WAXD and SAXS photographs of samples A and B at room temperature. The WAXD patterns of the two samples are characterized by (i) a very strong spot on the equator and (ii) diffuse and somewhat streaky reflections on the layer lines. Other equatorial reflections were too weak to be visible on the photographs. The streak diffractions on the layer lines can be related to the irregular alternation (intrachain disorder). More streaky layer line diffraction with discrete reflections on the equator was observed in poly( $\beta$ -propiolactone) *form II* crystal<sup>6</sup>. This kind of WAXD pattern can be caused by a disorder along the chain axis. In the latter case, however, the disorder is caused by the irregularity of the mutual levels of the chains, which has a regular structure, along the fibre axis (interchain disorder). The SAXS of sample A is layer-like, while that of sample B is spot-like. This difference indicates that the lateral dimension of crystals is much larger in sample B than in sample A.

*Figure 2* shows the equatorial WAXD intensity curves of the two samples. Sample A shows an asymmetric single peak with the maximum at about  $2\theta = 19^\circ$ . This asymmetry suggests a doublet character of the peak. Sample B shows two distinct peaks, which have their maxima at  $19^\circ$  and  $21^\circ$ . The profiles of dotted lines in *Figure 2* are obtained by using a Pearson type VII distribution function that was used by Heuvel *et al.*<sup>7</sup> in the analysis of WAXD profiles of nylon-6. The most significant feature observed from the WAXD profile of sample A is the paracrystalline disorder in the lateral packing of the chains, which was already present in the original sample and could not be removed by drawing and the subsequent annealing. It should be noticed that

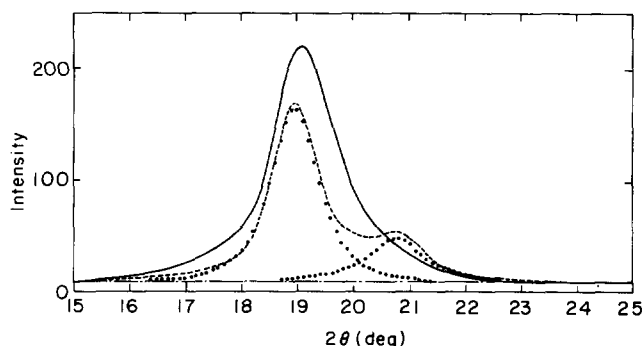


**Figure 2** Equatorial WAXD intensity curves at room temperature. Solid line is for sample A and broken line is for sample B. The two diffraction peaks given by dotted lines are those separated from the profile of sample B by using a Pearson type VII function. The peak at  $2\theta = 18.94^\circ$  is the 120 reflection and that at  $2\theta = 20.74^\circ$  the 200 reflection

the paracrystal tends to have a pseudo-hexagonal packing, which shows only one intense reflection  $(100)_h$  on the equator. On the other hand for sample B the crystallization under molecular orientation proceeds with a small number of oriented nuclei and the molten free chains grow on the nuclei to ordered crystals. Figure 3 shows the equatorial WAXD intensity curve of sample B at Bragg angles beyond those shown in Figure 2. The intensity is very low beyond  $2\theta = 30^\circ$ .

Figure 4 shows the meridional WAXD intensity curve of sample B. The same meridional curves as for sample B were obtained for other samples. This means that the chain conformation and the mutual levels of the chains do not depend so much on the method of preparation altering the lateral packing of the chains. Four peaks at  $2\theta = 18^\circ, 37^\circ, 55^\circ$  and  $76^\circ$  are the  $00l$  ( $l=1-4$ ) reflections, respectively.

#### Crystal structure

**Molecular conformation.** The fibre identity period was estimated to be  $5.04 \text{ \AA}$  from the meridional  $004$  reflection

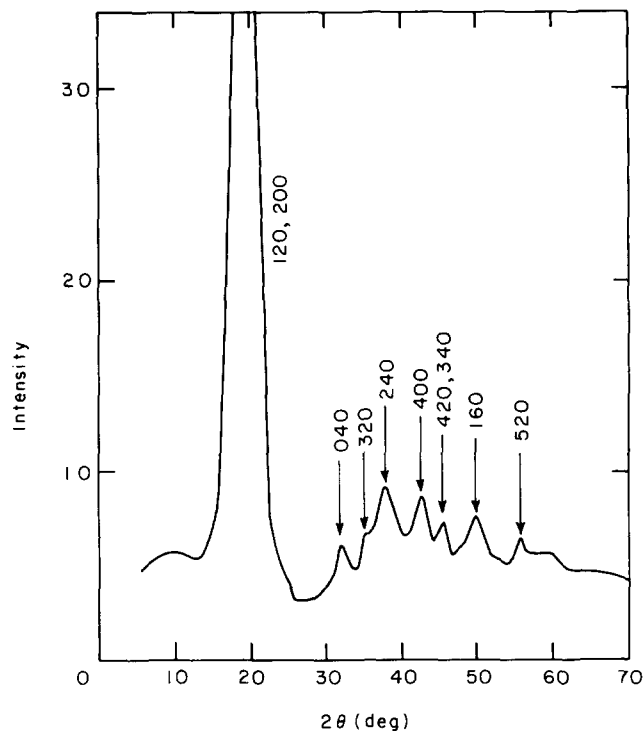


Figure 3 Equatorial WAXD intensity curve of sample B at wide angle of  $2\theta$

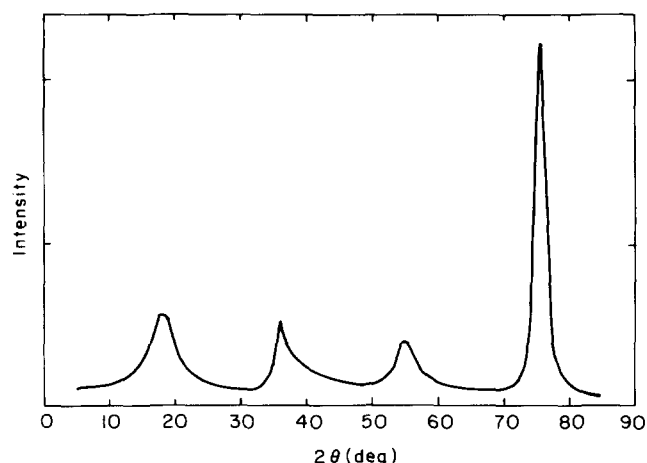


Figure 4 Meridional WAXD intensity curve of sample B

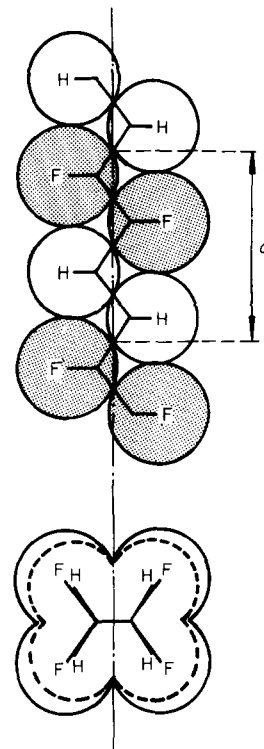
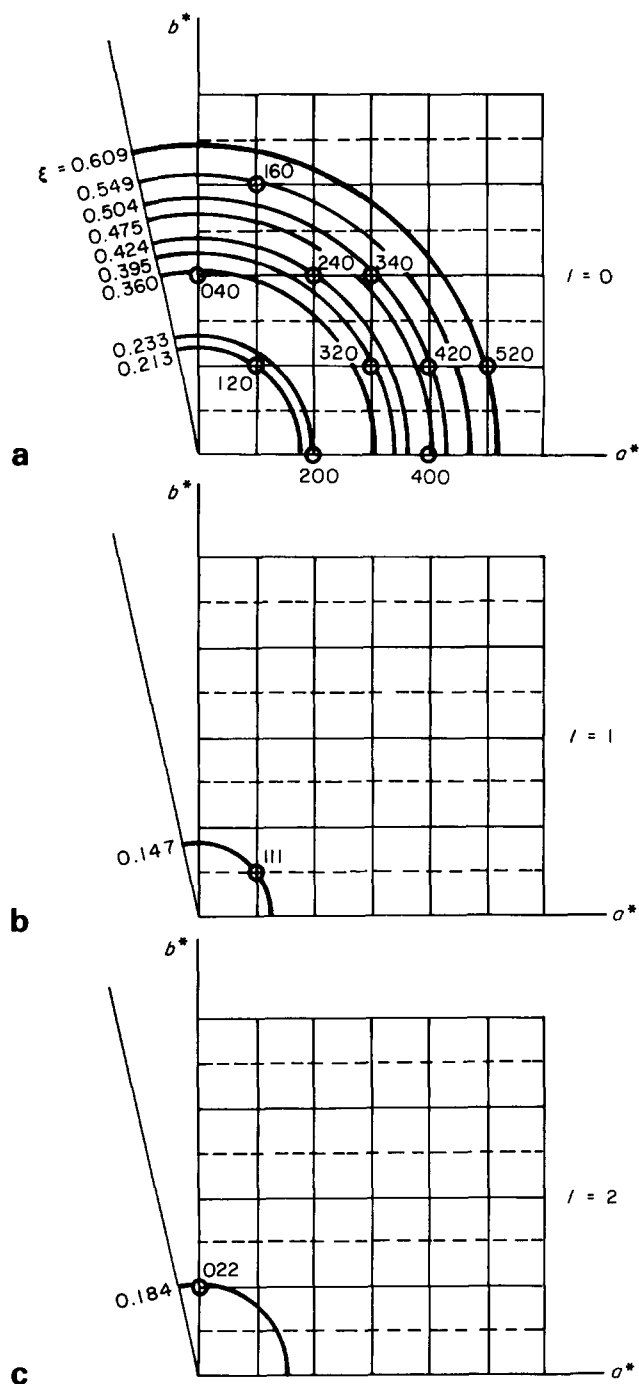


Figure 5 Molecular conformation of regular alternating ETFE copolymer. The fibre period ( $c$ -dimension) derived from the meridional  $004$  reflection in Figure 4 is consistent with the linear arrangement of fluorine and hydrogen atoms along its planar zigzag skeletal chain, as shown by the molecular model

observed for sample B. The same value has already been reported by Wilson and Starkweather<sup>1</sup>. This  $c$ -dimension implies a planar zigzag conformation of the chains, as shown in Figure 5. For the chain with regular alternation, the alternative location of fluorine and hydrogen atoms along the chain axis does not make any deflection from its planar conformation, because of their good conformity in size with the C-C periodic distance.

**Unit cell.** The equatorial reflections of sample B seem to be similar to those of the orthorhombic PE crystal. The ratio of intensities and the relative positions in Bragg angle of the two strongest reflections are analogous to the  $110$  and  $200$  reflections of PE. By referring to the unit cell of PE, all the equatorial and the second layer line reflections can be well indexed by a rectangular reciprocal lattice with  $a^* = 0.117 \text{ \AA}^{-1}$  and  $b^* = 0.179 \text{ \AA}^{-1}$  ( $= b'^*$ ), as illustrated by solid lines in Figure 6. This lattice corresponds to a real cell with  $a = 8.57 \text{ \AA}$  and  $b' = 5.60 \text{ \AA}$ , which is denoted as the sub-cell. However, when the sub-cell is adopted, the first layer line reflection is indexed as the  $1, 1/2, 1$ . This reflection can be exactly indexed when the  $b^*$ -dimension is reduced to half that in the initial reciprocal lattice ( $b^*$ ), as illustrated by the lattice that is composed of solid lines and broken ones in Figure 6. Therefore, the  $b$ -dimension of the real unit cell should be taken to be twice as large as that of the sub-cell. Thus, we propose here the orthorhombic unit cell with  $a = 8.57 \text{ \AA}$ ,  $b = 11.20 \text{ \AA}$  and  $c = 5.04 \text{ \AA}$ . It is noted that only one reflection necessitates the enlargement of the unit cell to be indexed as  $111$ .

**Crystal density.** By assuming that the copolymer composition of  $\text{CH}_2\text{CH}_2/\text{CF}_2\text{CF}_2$  is 50/50 mole%, and that four chemical repeating units ( $\text{CH}_2\text{CH}_2\text{CF}_2\text{CF}_2$ ) are



**Figure 6** Diffractions observed on the reciprocal lattice: (a) on the equator; (b) on the first layer; (c) on the second layer.  $\zeta$  is the radius in a reciprocal cylindrical coordinate

included in the unit cell, the calculated density of the crystal phase is  $1.757 \text{ g cm}^{-3}$ . The number of included chains is considered to be reasonable from the view of steric hindrance between the molecules. However, the value of the density is unreasonable, because it is almost the same as the observed density of sample B ( $1.76 \text{ g cm}^{-3}$ ). As we will report in our next paper<sup>8</sup>, the actual copolymer composition is derived to be 47.3/52.7 mole% from a dilatometric study. This composition implies the chemical repeating unit  $(\text{CH}_2\text{CH}_2)_{0.946}(\text{CF}_2\text{CF}_2)_{1.054}$ . The calculated crystal density was found to be  $1.807 \text{ g cm}^{-3}$ . Further, the crystallinity of sample B is 65%, by using the density of the amorphous phase ( $1.684 \text{ g cm}^{-3}$ )<sup>8</sup>. As the mole fraction of

the tetrafluoroethylene unit is slightly larger than 0.5, the densities are larger than those expected for the regularly alternating copolymer. This deviation is also supported by the melting point of this copolymer by comparison with the regular one. According to the reported relation between the melting point and the composition<sup>4</sup>, the melting point of our samples ( $267^\circ\text{C}$ ) indicates  $\pm(2-4)$  mole% deviation. The irregular chain structure together with the disordered packing of the chains can be easily inferred from the deviation of the composition alone.

**Molecular packing in the *ab*-plane.** Since the discrete reflections were too few to make detailed analysis of molecular packing, the projected structure onto the *ab*-plane was estimated by the following convenient method. First, it was assumed that planar zigzag chains with perfect alternating order were arranged in the unit cell as in the orthorhombic PE crystal. Then the 120 and 200 structure factors were calculated as a function of the setting angle  $\phi$  between the *b*-axis and the molecular plane. The following values of bond lengths and bond angles were used in the calculation: C-C =  $1.54 \text{ \AA}$ , C-F =  $1.34 \text{ \AA}$ , C-H =  $1.09 \text{ \AA}$ , C-C-C =  $109.5^\circ$ , F-C-F =  $109^\circ$ , and H-C-H =  $112^\circ$ . The intensity ratio of 120 to 200 thus calculated was compared with the observed value, 2.7. They became equal at  $\phi = 27^\circ$  and  $45^\circ$ . Since an orthorhombic cell with  $a = 7.0 \text{ \AA}$  and  $b = 5.5 \text{ \AA}$  was reported to have the lowest packing energy at  $\phi = 46^\circ$  (ref. 5), we preferred  $45^\circ$  to  $27^\circ$  as the setting angle. The sub-cell of our unit cell corresponds to their cell.

The molecular packing thus estimated is shown in Figure 7, where the van der Waals radii of C, F and H atoms are taken as  $2.0 \text{ \AA}$ ,  $1.35 \text{ \AA}$  and  $1.2 \text{ \AA}$ , respectively. The mutual levels of ethylene (E) and tetrafluoroethylene

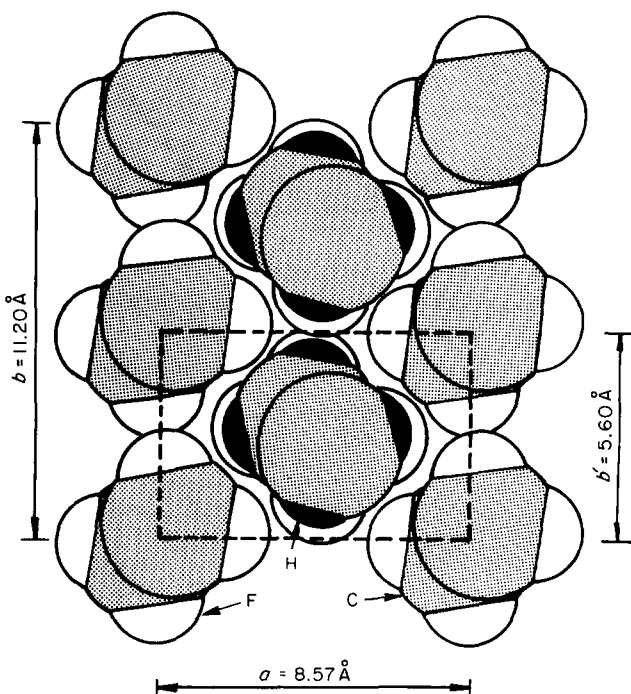


**Figure 7** Projection of the crystal structure of ETFE viewed along the *c*-axis. The setting angle ( $\phi$ ) is  $45^\circ$ . Broken lines represent the sub-cell with  $a = 8.57 \text{ \AA}$  and  $b' = 5.60 \text{ \AA}$ . Although the actual chain has much irregularity in the alternation of the two monomer units, we drew an unreal chain with perfect alternating order. It is not possible to illustrate the irregularity with such a small number of chains

(TFE) units between the neighbouring chains along the chain are illustrated according to Farmer and Lando's idea: TFE and ET units are located at the four corners and at the centre of the sub-cell, respectively. In the particular case of such a regular molecule with the regular alternation of the two monomer units as shown in the figure, the sub-cell is to be regarded as a unit cell for the crystal. However, the actual copolymer molecules made the unit cell twice as large as the sub-cell for their irregular alternation. For molecules with intrachain disorder, the determination of the unit structure in three dimensions is sometimes meaningless. From this point of view, our unit cell should be considered just as a convenience derived for indexing the reflections. So it would also be reasonable for the sub-cell to be regarded as a unit cell and the first layer line reflection to be treated as special due to the irregularity. Furthermore, it may be preferable to use an energy analysis while considering the irregularity. An illustration of the irregular structure thus derived can not be drawn by such a small number of chains as shown in *Figure 7*. Contrary to these discussions, we drew, as a reference structure, the observed unit cell and the molecules with perfect alternation. However, as far as the projected structure onto the *ab*-plane is concerned, it is allowed to take the sub-cell as the unit structure.

The chains seem to be rather loosely packed in *Figure 7*, particularly in the *a*-axis direction. This may result from the fact that the lattice is expanded by steric hindrance between such bulky TFE units as mislocated at the same level along the chain axis by the irregular alternation. This assumption also explains the reason why the observed *a*-axis dimension is much larger than that expected on the calculation of Farmer and Lando<sup>5</sup>.

**Double orientation.** Although the paracrystal in sample A seemed to be pseudo-hexagonal as described above, its intrinsic structure would be the same as the orthorhombic structure observed in sample B. The asymmetric nature of the profile of sample A in *Figure 2*, which is trailing the larger  $2\theta$  angle, provided us with one reason to reexamine the mode of double orientation of the crystals. For this purpose two kinds of doubly oriented samples R and AR were prepared.

WAXD and SAXS photographs are shown for samples R and AR in *Figures 9* and *10*, respectively. A coordinate system *X*, *Y* and *Z* is fixed to each sample as shown in *Figure 8*, where *X* is the transverse direction, *Y* the thickness direction, which is normal to the film plane (rolled plane), and *Z* the drawing and/or rolling direction. No substantial difference between the corresponding photographs is found with the exception of *9c* and *10c*, where we can read some differences in the degree of crystal orientation and of the azimuthal angles of the reflections. The difference in the degree of orientation is not important here. Six spots on a concentric circle appear in *Figures 9c* and *10c* with different azimuthal angles, i.e.  $\psi = 30^\circ + 60^\circ n$  in *Figure 9* and  $\psi = 0^\circ$  and  $60^\circ n$  in *Figure 10*, where *n* is an integer.

To assign these six spots on the end-view pattern, the intensity profiles at  $\psi = 30^\circ$  and  $90^\circ$  in sample R and those at  $\psi = 0^\circ$  and  $60^\circ$  in sample AR were measured by using the X-ray diffractometer as shown in *Figures 11* and *12*, respectively. No significant difference is found between the two profiles in *Figure 11*, while a large difference is found between those in *Figure 12*. Namely, the profile at  $\psi = 0^\circ$  shown by a broken line has a shoulder at

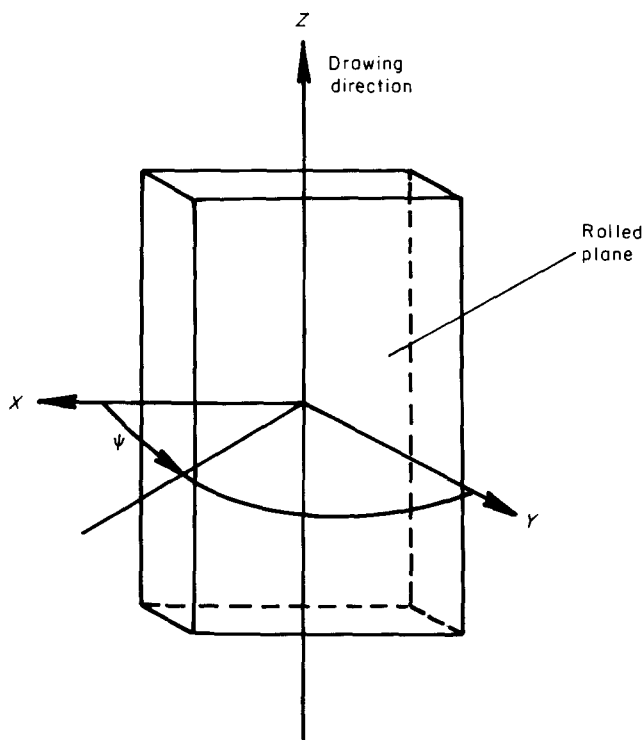


**Figure 8** Definition of a coordinate system fixed to a specimen film: *X* is the transverse direction, *Y* the thickness direction (normal to the film plane) and *Z* the drawing and/or rolling direction. An optional direction in the *XY*-plane is designated by the angle  $\psi$

$2\theta = 20.75^\circ$  in addition to a peak at  $2\theta = 19.27^\circ$  as indicated by dotted lines, while the profile at  $\psi = 60^\circ$  has a single peak at  $2\theta = 19.10^\circ$ . By the crystal unit cell determined above, both peaks at  $2\theta = 19.10^\circ$  and  $19.27^\circ$  are identified as the 120 reflection, and the peak at  $2\theta = 20.75^\circ$  as the 200 reflection. The slight difference in the peak angles of the 120 reflections may be due to a difference in the degree of packing order caused by rolling.

These end-view patterns are very similar to those of rolled PE, suggesting a close similarity in the crystal structures of PE and ETFE. These findings lead us to assign the six-spot patterns shown in *Figures 13a* and *13b*. In these figures the solid lines and the broken lines represent the sub-cell and the reciprocal lattice, respectively. The relation between a pair of the cell and the lattice is illustrated in *Figure 13c*. The 200 and 120 reflections are indicated separately by the same marks in *Figure 13*, although these reflections are observed for samples R and AR as a doublet with a much weaker 200 reflection than a 120 one. According to Frank *et al.*<sup>9</sup> and Seto *et al.*<sup>10</sup>, the (110) and (100) slips and the (110) and (310) twinings take place by the rolling of PE. The same modes of deformation as in PE can be seen in ETFE. However, we will not discuss this deformation mechanism in detail. Here, the important fact is that the two types of crystal orientation are both found in the two samples R and AR: types P and Q (Q') in sample R and types S and R (R') in sample AR. In the former sample the two types of orientation occur with almost the same proportion so that the doublet of 120 and 200 reflections appears uniformly at the six points. On the other hand, type S crystal orientation is dominant in sample AR. Thus the weaker reflection of 200 can be observed as a shoulder on the WAXD intensity curve at  $\psi = 0^\circ$  in *Figure 12*. The 120 and 200 reflections on this curve are attributed to the crystals with different types of orientation: the former to

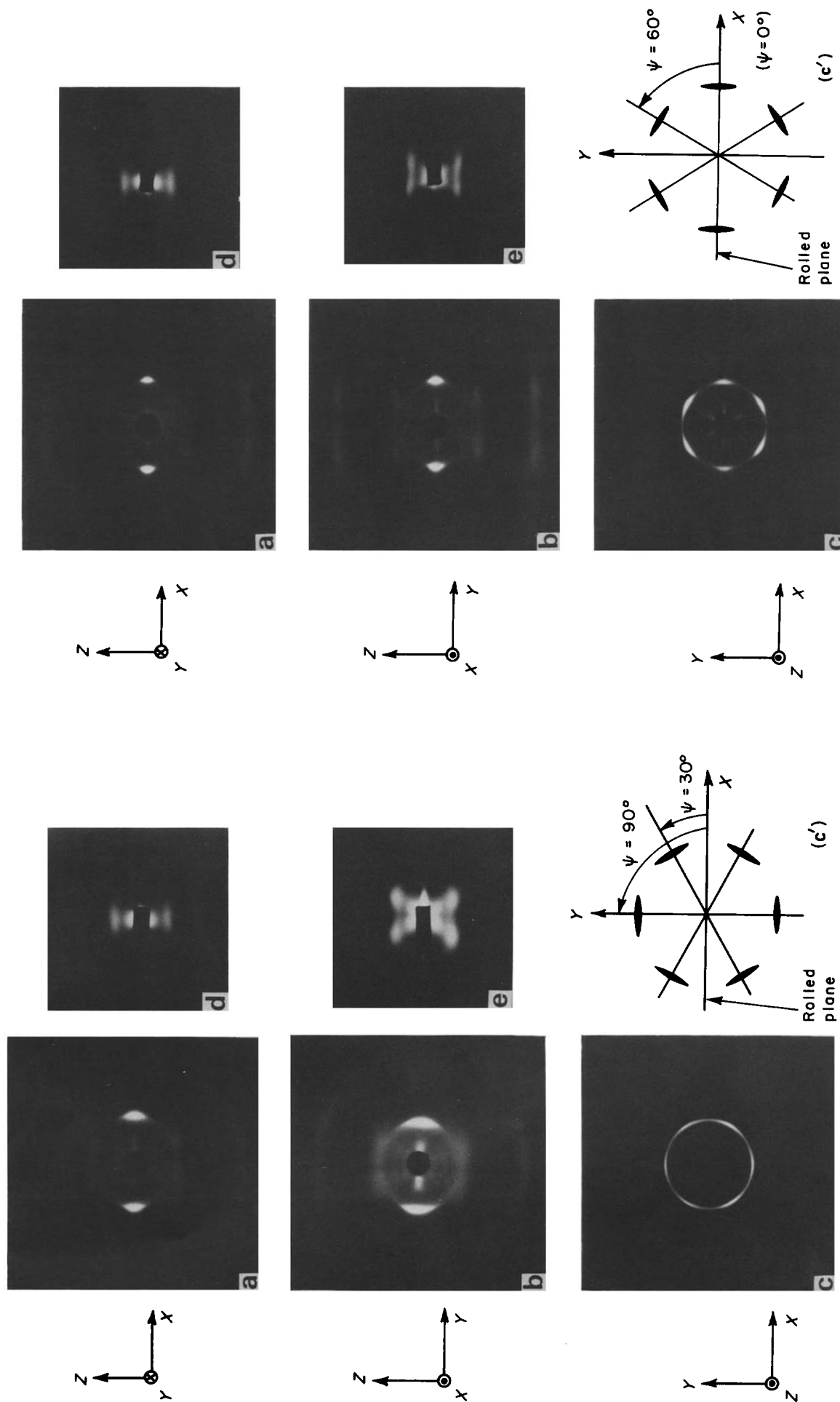


Figure 9 (a)-(c) WAXD and (d), (e) SAXS photographs of the rolled sample (sample R) along the axes indicated. (c') The schematic representation of (c)

Figure 10 (a)-(c) WAXD and (d), (e) SAXS photographs of the drawn-rolled sample (sample AR) along the axes indicated. (c') The schematic representation of (c)

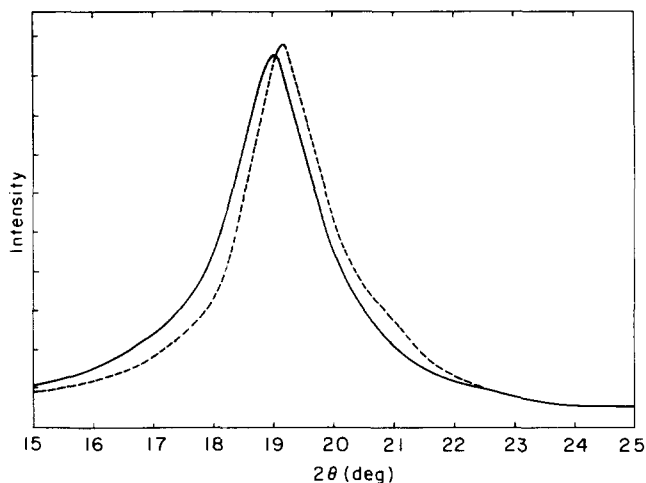


Figure 11 Equatorial WAXD intensity curves of sample R (—)  $\psi = 90^\circ$ , (---)  $\psi = 30^\circ$

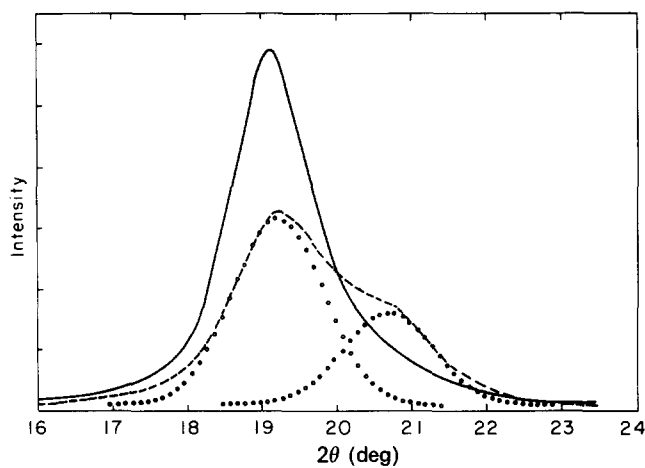


Figure 12 Equatorial WAXD intensity curves of sample AR (—)  $\psi = 60^\circ$ , (---)  $\psi = 0^\circ$

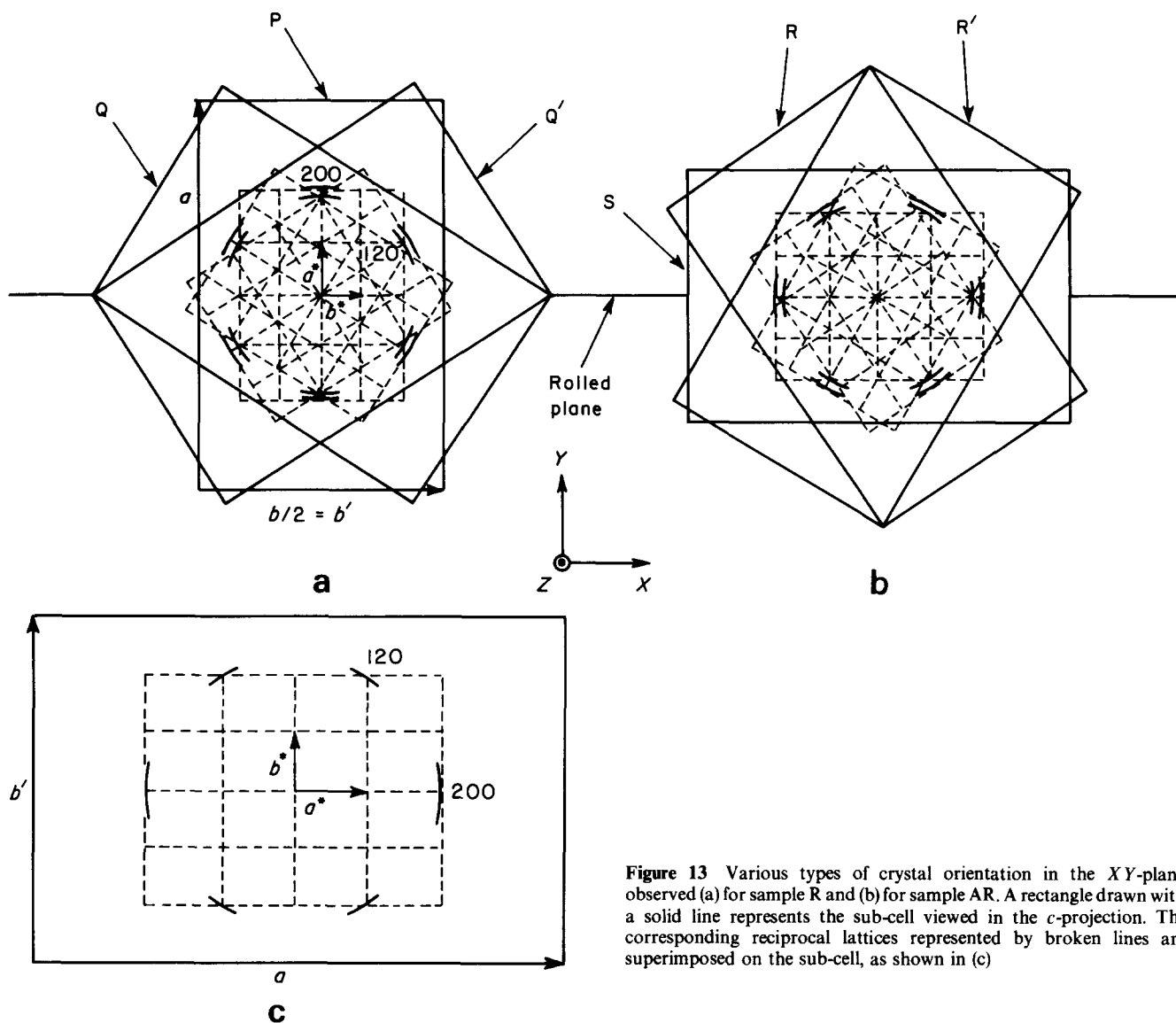


Figure 13 Various types of crystal orientation in the  $XY$ -plane observed (a) for sample R and (b) for sample AR. A rectangle drawn with a solid line represents the sub-cell viewed in the  $c$ -projection. The corresponding reciprocal lattices represented by broken lines are superimposed on the sub-cell, as shown in (c)

type S and the latter to type R. Wilson and Starkweather<sup>1</sup> used a drawn and rolled ETFE sample that seems to have the same character as our sample AR. Unfortunately they did not mention the  $21^\circ$  peak (our 200 reflection), although it appeared in their data (Figure 2 in ref. 1). They noticed only the type P orientation mode.

As described above, the double orientation explains that the orthorhombic crystal proposed for sample B can also be found in the disordered structure in sample A, and that the molecular packing mode in ETFE crystal is very similar to that in PE. Further, as well as the crystal orientation mode, the packing order of the chains in the

*ab*-plane is much affected by rolling. The type S crystal, which seems to be most heavily deformed, shows higher packing order than the other crystals. Thus the appearance of the orthorhombic crystal may be attributed partly to the ordering in the rolling process, as well as to the effect of the double orientation. As a result, the pseudo-hexagonal structure of sample A seems to be based on orthorhombic packing, although it is very disordered.

## CONCLUSIONS

The highly ordered crystal of ETFE was obtained by crystallization from the melt under extension (sample B). Although its crystal structure is in the highest ordered state compared with other ETFE samples, such as our sample A, the intrinsic disorder due to the irregular alternation of the two monomer units can not be removed.

The crystal structure was determined by using sample B. The unit cell was orthorhombic with the following dimensions:  $a=8.57 \text{ \AA}$ ,  $b=11.20 \text{ \AA}$  and  $c$  (fibre axis)  $=5.04 \text{ \AA}$ , in which four planar zigzag chains were contained. The lateral packing mode of the chains in the unit cell was very similar to that in PE. It was not possible to determine the unit structure in three dimensions, which is usually displayed in other homopolymers, because of the irregular alternating order in the chain. Further, the irregularity can not be illustrated by such a small number of chains as shown in *Figure 7*. But, we dare to use (as a

desperate measure!) the chain with the perfect alternation order for the illustration of the observed unit cell.

From the doubly orientated modes it was confirmed that the pseudo-hexagonal structure in sample A was also the orthorhombic one, possessing a rather paracrystalline nature. The modes also showed that the packing style of the chains in ETFE is similar to that in PE.

## ACKNOWLEDGEMENT

We are indebted to Asahi Glass Co. Ltd. for providing the samples, and to Dr Takashi Inoue (Tokyo Institute of Technology) for his help in preparing the manuscript.

## REFERENCES

- 1 Wilson, F. C. and Starkweather, H. W. Jr. *J. Polym. Sci., Polym. Phys. Edn.* 1973, **11**, 919
- 2 Modena, M., Garbuglio, C. and Ragazzini, M. *J. Polym. Sci., Polym. Lett. Edn.* 1972, **10**, 153
- 3 Koyama, R. and Satokawa, T. *Yuki Gosei Kagaku Kyokaishi* 1973, **31**, 518
- 4 Yamabe, M., Miyake, M., Ukihashi, H. and Tabata, Y. *Rep. Res. Lab. Asahi Glass Co. Ltd.* 1973, **23**, 61
- 5 Farmer, B. L. and Lando, J. B. *J. Macromol. Sci.-Phys.* 1975, **B11**, 89
- 6 Suehiro, K., Chatani, Y. and Tadokoro, H. *Polym. J.* 1975, **7**, 352
- 7 Heuvel, H. W., Huisman, R. and Lind, K. C. J. B. *J. Polym. Sci., Polym. Phys. Edn.* 1976, **14**, 921
- 8 Tanigami, T. *et al.*, to be published
- 9 Frank, F. C., Keller, A. and O'Connor, A. *Phil. Mag.* 1958, **8**, 64
- 10 Seto, T., Hara, T. and Tanaka, H. *Jpn. J. Appl. Phys.* 1968, **7**, 31